Molecular Biology of the Cell
Vol. 20, 1241–1251, February 15, 2009

# Deficient SUMO Attachment to Flp Recombinase Leads to Homologous Recombination-dependent Hyperamplification of the Yeast 2 μm Circle Plasmid

**Ling Xiong,* Xiaole L. Chen,* Hannah R. Silver, Noreen T. Ahmed, and Erica S. Johnson**

Department of Biochemistry and Molecular Biology, Thomas Jefferson University, Philadelphia, PA 19107

Submitted June 30, 2008; Revised November 18, 2008; Accepted December 8, 2008
Monitoring Editor: Charles Boone

**Many *Saccharomyces cerevisiae* mutants defective in the SUMO pathway accumulate elevated levels of the native 2 μm circle plasmid (2 μm). Here we show that accumulation of 2 μm in the SUMO pathway mutants *siz1*Δ *siz2*Δ, *slx5*Δ, and *slx8*Δ is associated with formation of an aberrant high-molecular-weight (HMW) form of 2 μm. Characterization of this species from *siz1*Δ *siz2*Δ showed that it contains tandem copies of the 2 μm sequence as well as single-stranded DNA. Accumulation of this species requires both the 2 μm–encoded Flp recombinase and the cellular homologous recombination repair (HRR) pathway. Importantly, reduced SUMO attachment to Flp is sufficient to induce formation of this species. Our data suggest a model in which Flp that cannot be sumoylated causes DNA damage, whose repair via HRR produces an intermediate that generates tandem copies of the 2 μm sequence. This intermediate may be a rolling circle formed via break-induced replication (BIR), because mutants defective in BIR contain reduced levels of the HMW form. This work also illustrates the importance of using cir° strains when studying mutants that affect the yeast SUMO pathway, to avoid confusing direct functions of the SUMO pathway with secondary effects of 2 μm amplification.**

## INTRODUCTION

The 2 μm circle is a naturally occurring 6318-base pair plasmid (2 μm) present in ~40–60 copies in virtually all strains of *Saccharomyces* (Broach and Volkert, 1991). 2 μm's only known activity is self-propagation, which is accomplished via two distinct plasmid maintenance mechanisms (Jayaram *et al.*, 2004). One of these allows the plasmid to be amplified if its copy number drops and is mediated by the plasmid-encoded Flp recombinase and two DNA target sites for Flp (FRT) that are present on opposite sides of the plasmid. Flp catalyzes an intramolecular recombination reaction between the two FRT sites, thereby inverting one side of the 2 μm with respect to the other. Futcher (1986) has proposed a model that explains how this activity could allow multiple copies of 2 μm to be made from a single origin firing: if recombination occurs during replication between the converging replication forks (RFs), it would generate a double rolling circle where both forks chase each other around the template in the same direction. The 2 μm sequence would be rereplicated until a second Flp-dependent recombination event permits convergence of the RFs.

Native levels of 2 μm have little effect on the growth rate of wild-type (wt) yeast (Broach and Volkert, 1991). However, in several mutants defective in the SUMO (Smt3) pathway, accumulation of high copy numbers of 2 μm is associated with slow, cold-sensitive growth, and cell cycle delays caused by activation of the DNA damage checkpoint (Zhao *et al.*, 2004; Chen *et al.*, 2005; Dobson *et al.*, 2005; Burgess *et al.*, 2007; Ii *et al.*, 2007b). These strains are also heterogeneous and form irregularly shaped colonies, presumably because different lineages contain different levels of 2 μm, leading to different degrees of growth inhibition. Removal of 2 μm from these strains eliminates these conspicuous growth defects.

SUMO is a ubiquitin-like protein that functions by being attached to other proteins as a posttranslational modification (Johnson, 2004; Hay, 2005; Geiss-Friedlander and Melchior, 2007). SUMO conjugation is essential for viability of *Saccharomyces cerevisiae*, and SUMO is attached to hundreds of yeast proteins. SUMO attachment is catalyzed by a three-step pathway analogous to the ubiquitin pathway. In yeast, the SUMO pathway consists of the heterodimeric E1 Uba2-Aos1, the E2 Ubc9, and several SUMO ligases (E3s), which include Siz1, Siz2/Nfi1, Mms21, and the meiotic E3 Zip3 (Geiss-Friedlander and Melchior, 2007). SUMO can be cleaved off substrate proteins by SUMO-specific proteases, including the yeast Ulp1 and Ulp2. Ulp1 is also required for maturation of the SUMO precursor and so participates in both SUMO conjugation and deconjugation. Mutants in certain nuclear pore complex (NPC) and nuclear envelope proteins also have sumoylation defects because they mislocalize Ulp1 (Zhao *et al.*, 2004; Chen *et al.*, 2007; Lewis *et al.*, 2007; Palancade *et al.*, 2007). Recently, a factor that acts down-

This article was published online ahead of print in *MBC in Press* (http://www.molbiolcell.org/cgi/doi/10.1091/mbc.E08–06–0659) on December 24, 2008.

* These authors contributed equally to this work.

Address correspondence to: Erica S. Johnson (erica.johnson@jefferson.edu).

Abbreviations used: 2 μm, yeast 2-μm circle plasmid; BIR, break-induced replication; DSB, double-strand break; EtBr, ethidium bromide; FRT, Flp recombination target; GFP, green fluorescent protein; HJ, Holliday junction; HMW, high molecular weight; HRR, homologous recombination repair; NPC, nuclear pore complex; QAOS, quantitative analysis of single-stranded DNA; RF, replication fork; ssDNA, single-stranded DNA; wt, wild-type.

stream of sumoylation has been identified: a heterodimer consisting of Slx5/Hex3, and Slx8 acts as a ubiquitin ligase that targets sumoylated proteins for ubiquitin-dependent proteolysis (Ii *et al.*, 2007a; Prudden *et al.*, 2007; Sun *et al.*, 2007; Uzunova *et al.*, 2007; Xie *et al.*, 2007). The natural substrates of Slx5·Slx8-dependent ubiquitylation are unknown.

The *siz1*Δ *siz2*Δ double mutant, *slx5*Δ, *slx8*Δ, *ulp1*, and certain NPC mutants accumulate as much as 10-fold higher than wt levels of 2 μm DNA (Zhao *et al.*, 2004; Chen *et al.*, 2005; Dobson *et al.*, 2005; Burgess *et al.*, 2007; Ii *et al.*, 2007b). A potential mechanism for SUMO's role in 2 μm stability is suggested by the fact that Flp recombinase is modified by SUMO at a fairly high level (~10%; Chen *et al.*, 2005). When Flp sumoylation is reduced, either in the *siz1*Δ *siz2*Δ mutant or in a strain where *FLP* is mutated to eliminate its major SUMO attachment site, Flp protein accumulates to higher than wt levels (Chen *et al.*, 2005). These higher levels of Flp could be partially responsible for hyperamplification of 2 μm, because overexpression of Flp also increases 2 μm DNA levels (Murray *et al.*, 1987; Reynolds *et al.*, 1987).

Here we found that the 2 μm hyperamplification in SUMO pathway mutants requires the homologous recombination repair (HRR) pathway. During vegetative yeast growth, the primary role of HRR is to repair double-strand breaks (DSBs) and to resolve aberrant structures generated during DNA replication (Paques and Haber, 1999; Krogh and Symington, 2004). The *RAD52* epistasis group is responsible for carrying out HRR and includes genes involved in several distinct processes. The *RAD51* subgroup: *RAD51*, *RAD52*, *RAD54*, *RAD55*, and *RAD57*, is required for gene conversion events, which require participation of both sides of the DSB in the repair reaction. The *RAD51* group can also carry out break-induced replication (BIR), where one end of a DSB invades an intact homologous sequence and establishes a RF that performs both leading and lagging strand synthesis and can copy many kilobases of DNA (McEachern and Haber, 2006; Llorente *et al.*, 2008). This process involves only one side of the DSB. BIR can also take place by a *RAD51*-independent mechanism that involves *RAD52*, *RAD59*, *RDH54/TID1*, and the *MRE11-RAD50-XRS2* complex (MRX). Mutants lacking both known BIR pathways dramatically reduce, but do not entirely eliminate, BIR (McEachern and Haber, 2006; Llorente *et al.*, 2008), suggesting that there are additional BIR mechanisms.

There is no evidence that HR participates in the normal Flp-dependent amplification of 2 μm in wt cells. In vitro, Flp is sufficient to carry out recombination between two FRT sequences (Grainge and Jayaram, 1999). However, experiments using engineered constructs have shown that Flp activity can lead to Rad52-dependent recombination in yeast (Prado *et al.*, 2000; Storici and Bruschi, 2000). Furthermore, Flp's catalytic mechanism suggests how it could form a DSB. Flp and related recombinases initiate their catalytic reaction by forming a single-strand break in the DNA target site, where the active site Tyr of the recombinase is covalently linked to the 3′ phosphate of the broken strand (Grainge and Jayaram, 1999). This feature of recombinase activity is similar to the mechanism of type IB topoisomerases such as eukaryotic topoisomerase I (Top1), which form similar covalent intermediates and cause DSBs when these covalent intermediates are encountered by RFs (Li and Liu, 2001; Pommier, 2006; Koster *et al.*, 2007).

Here we have investigated the mechanism of 2 μm hyperamplification in SUMO pathway mutants and have found that it requires both Flp and HRR. Our results suggest a model in which deficient sumoylation of Flp results in Flp-dependent DNA damage, whose repair via HRR leads to formation of a species that generates multiple tandem copies of the 2 μm DNA sequence.

## MATERIALS AND METHODS

### *Media and Genetic Techniques*

Standard techniques were used (Ausubel *et al.*, 2000). Rich yeast medium containing 2% glucose (YPD) and synthetic yeast medium were prepared as previously described (Sherman *et al.*, 1986). Galactose inductions were done by adding 2% galactose to cells pregrown in YP containing 2% raffinose. Cell cycle arrests were done using 10 μM α factor or 15 μg/ml nocodazole.

### *Plasmid and Yeast Strain Constructions*

*S. cerevisiae* strains used are listed in Supplemental Table S1. Mutations and C-terminal green fluorescent protein (GFP) or epitope tags were introduced into native loci in chromosomal sequences or native 2 μm by transforming strains with appropriate PCR products, as described (Johnson and Blobel, 1999). For modifications of native 2 μm, once a strain containing the correct plasmid was obtained, whole genomic DNA from this strain was transformed into appropriate cir° strains to obtain strains containing only the modified 2 μm plasmid (Chen *et al.*, 2005). The sequence of the hemagglutinin (HA)-$His_8$ tag on Flp and mutant derivatives was GYPYDVPDYAAFLHHHHH-HHH. Oligonucleotide sequences are available on request. A CEN-based plasmid expressing untagged Flp from a *GAL1* promoter was constructed by inserting the Flp coding region into p415*GAL1* (Mumberg *et al.*, 1994).

### *Analysis of 2 μm Species*

Total levels of 2 μm DNA were measured using quantitative PCR (qPCR) as described (Chen *et al.*, 2005), using DNA prepared by glass-bead lysis (Hoffman and Winston, 1987). DNA for Southern blotting was prepared either by a different glass-bead lysis protocol (Adkins and Tyler, 2004) where DNA was treated with 50 μg/ml proteinase K (Figure 3) or by spheroplasting and lysing cells in denaturing conditions as described (Holm *et al.*, 1986; Figures 4, 5, B and C, 6, and 8) with the following modifications: the preparation was treated with RNase at the end of the protocol rather than before the proteinase K step, and the suspension was brought to a concentration of 0.5% SDS before proteinase K treatment. These protocols give somewhat different relative levels of 2 μm DNA between wt and SUMO mutant cells, with glass-bead methods showing a greater apparent difference. This is because the Holm *et al.* (1986) method produces greater yields of the 2 μm DNA from wt cells (not shown). Chloroquine gels (Figure 3) contained 1.2% agarose and 0.75 μg/ml chloroquine and were run in 1× Tris-borate EDTA (TBE) at 2 V/cm for 24 h at RT (Adkins and Tyler, 2004). Ethidium bromide (EtBr) gels (Figures 4, 5, B and C, 6, A, C and D, and 8) contained 0.6% agarose and 0.3 μg/ml EtBr and were run in 1× TBE at 1–2 V/cm at 4°C for 16–20 h. The gel in Figure 6B contained 1.5% agarose and was run in 1× Tris-acetate EDTA (TAE) at 6 V/cm for 3 h. Lanes in Southern blots were normalized to contain equal amounts of 2 μm DNA, except in Figure 4D, where equal amounts of total DNA were loaded. Individual 2 μm species (Figure 5C) were isolated from EtBr gels made from low-melting point agarose by extracting melted gel slices with phenol and then 25:24:1 phenol/chloroform/isoamyl alcohol, followed by ethanol precipitation. Pulsed-field gel electrophoresis (Figure 5A) was performed using DNA prepared embedded in low-melting point agarose as described (Schwartz and Cantor, 1984). Approximately 20 μl per lane of agarose-embedded DNA was treated with PMSF in Tris-EDTA (TE; pH 8.0), washed with TE supplemented with New England Biolabs (Beverly, MA) buffer 3, melted, and digested to completion with BglII, which does not cleave in 2 μm, to reduce the chromosomal DNA to mostly small (<10 kb) fragments. This preparation was either loaded directly or digested with EagI, which cleaves once in 2 μm. To give partial or complete digests, reactions containing 0.2 or 1.0 U of EagI were incubated at 37°C for 30 min, or reactions containing 20 U were incubated for 2 h. About fivefold more total DNA preparation was loaded in the wt lanes than in *siz1*Δ *siz2*Δ lanes (because it was impossible to quantify 2 μm DNA by qPCR in these preparations, which contain unlysed cells and debris). Samples were analyzed by electrophoresis on a 1% agarose gel in 0.5× TBE in a Bio-Rad CHEF-DR II pulsed field electrophoresis system (Hercules, CA) at 200V (6 V/cm) for 19.2 h at 14°C with switch times ramped from 1 to 20 s. Southern transfers were performed as described (Ausubel *et al.*, 2000), and hybridizations (except Figure 6B) were done using a probe containing two PCR products containing base pairs 5953-1270 (including position 1) and 2120-4579 of 2 μm (numbering according to *Saccharomyces* Genome Database), labeled using the DIG High Prime Labeling Kit (Roche, Indianapolis, IN) according to the manufacturer's instructions. Probes in Figure 6B were prepared by the same method and contained base pairs 1327-1570 of 2 μm (probe A) and base pairs 1712-1946 (probe B). Chemiluminescent signals were quantified using a Bio-Rad Chemidoc gel documentation system. Restriction enzymes were from New England Biolabs.

### *Quantification of Single-stranded DNA in 2 μm by QAOS*

The QAOS method (quantitative analysis of single-stranded DNA [ssDNA]) was performed approximately as described (Booth *et al.*, 2001) and is illustrated in Supplemental Figure S2. For each reaction, a DNA sample containing a standard amount of 2 μm DNA (determined by qPCR) was digested with MboI and added to a reaction containing 0.4 pM tagging primer, 200 μM each dNTP, and 0.25 U/10 μl of Taq polymerase in PCR buffer (10 mM Tris, pH 8.85, 25 mM KCl, 5 mM $(NH_4)_2SO_4$, and 2 mM $MgCl_2$). This was incubated on ice for 5 min, at 25°C for 15 min, and at 37°C for 15 min. Different tagging primers were used to measure ssDNA on each strand (arbitrarily designated strands A and B) at a single locus. Ten microliters of this initial reaction was then included in 30-μl qPCR reactions made using the DyNAmo HS SYBR green qPCR kit (New England Biolabs). Two different qPCR reactions were performed for each initial reaction. One measured QAOS signal and contained the primer specific for the tag plus the appropriate flanking primer. The other measured total DNA at this locus.

Levels of ssDNA are indicated as the QAOS signal/total signal (measured as ΔCt and converted to a fraction). Three independent DNA preparations (made as described for total genomic DNA; Holm *et al.*, 1986) were analyzed for each strain; qPCR reactions were performed in duplicate. We do not believe that our QAOS qPCR reactions measured 100% of the ssDNA in a given sample, or, consequently, that the QAOS/total figure is a precise measurement of the fraction of a given sequence that is single-stranded. The QAOS signal seems likely to be substantially lower than the actual amount of ssDNA. It also appeared that different tagging primers gave somewhat different QAOS signals, and so it would be inappropriate to compare measurements made with different primers. (Thus, we cannot compare the levels of ssDNA on the different strands to each other.) However, this method can still be used to measure relative levels of ssDNA in different samples as long as the same primers are used. The tagging primers were 5′ TGCCCTCGCATCGCTCTCGAATTCCGTTG 3′ at position ~5690 in 2 μm for strand A and 5′ TGCCCTCGCATCGCTCTCGAAGCAAGT 3′ at position ~5863 for strand B. The tag primer was 5′ TGCCCTCGCATCGCTCTCGAA 3′ for both strands. The flanking primer for measuring strand A was 5′ AGAAGCAAGTCAGGCTGCCATAGA 3′ at 5872 and for strand B was 5′ ACATCTTCTTCCGTTGGAGCTGGT 3′ at position 5675. The flanking primers were used together to measure total DNA. qPCR was performed in a MJ Research (Waltham, MA) Opticon using cycles of 30 s at 95°C, 45 s at 55°C, and 2 min at 72°C. For analysis of isolated supercoiled and HMW species, bands were isolated from EtBr-stained low-melting agarose gels, and DNA was purified using β-agarase (New England Biolabs) as described by the manufacturer.

### *Antibodies and Immunoblot Analyses*

Yeast whole-cell lysates were prepared by lysis in NaOH (Yaffe and Schatz, 1984). HA and $His_8$-tagged proteins were purified from yeast by Ni-nitrilotriacetic acid (NTA) affinity chromatography (Chen *et al.*, 2005) and subjected to immunoblotting, followed by chemiluminescent detection (Johnson and Blobel, 1999). Antibodies were an affinity-purified rabbit polyclonal antibody (Ab) against Smt3 (SUMO; Johnson and Blobel, 1999), the 16B12 monoclonal Ab against the HA epitope (Covance Research Products, Denver, PA), and a rabbit polyclonal Ab against Flp, generously provided by M. Jayaram (University of Texas, Austin, TX). Photographs of immunoblots were made using chemiluminescent detection (Supersignal; Pierce, Rockford, IL). For quantification of signals, secondary antibodies coupled to fluorescent dyes IRDye 800 (Rockland Immunochemicals, Gilbertsville, PA) and Alexa Fluor 680 (Molecular Probes, Eugene, OR) were used with an Odyssey infrared imaging system (Li-Cor Bioscience, Lincoln, NE).

### *Microscopy*

Fluorescence micrographs were taken using a 63× oil objective on a Leica DM.RXA microscope (Deerfield, IL) with a Cool SNAP fx digital camera (Roper Scientific, Tucson, AZ) and IP Lab software (Scanalytics, Billerica, MA). Photomicrographs of yeast colonies were taken using a tetrad dissecting microscope with a 10× objective and 15× ocular by holding an Olympus Stylus 300 digital camera (Melville, NY) at 3× zoom to the ocular of the microscope.

## RESULTS

### *HRR Is Required for 2 μm Hyperamplification in* siz1Δ siz2Δ

We recently reported that a *siz1*Δ *siz2*Δ *rad52*Δ strain is nearly inviable, but that its growth defect is suppressed by deleting the gene encoding topoisomerase I (*TOP1*; Chen *et al.*, 2007). This phenotype is independent of 2 μm and is observed in strains both containing (cir$^+$) and lacking (cir°) 2 μm. However, this set of mutations also showed a separate

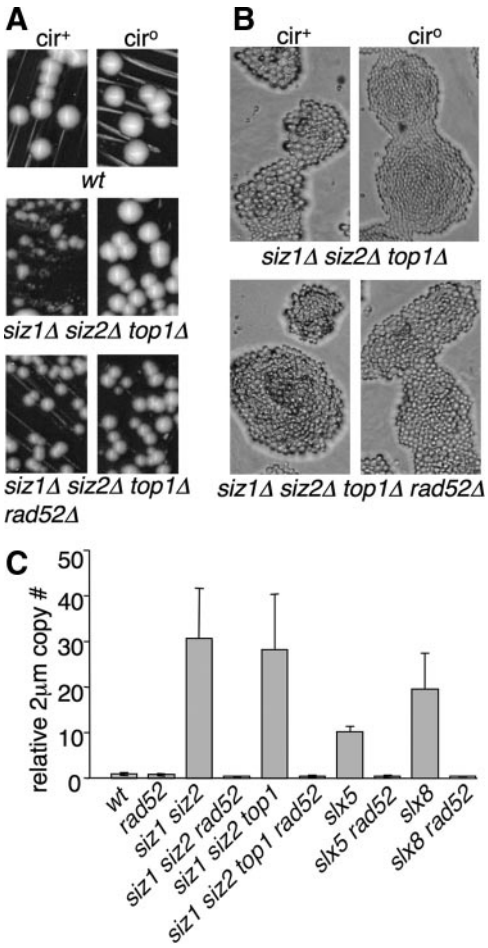


**Figure 1.** Hyperaccumulation of 2 μm requires homologous recombination. (A and B) Strains of the indicated genotypes were grown at 30°C on YPD plates for 2 d (A) or 1 d (B). Note that differences between cir° and cir$^+$ versions of *siz1*Δ *siz2*Δ *top1*Δ in both colony and cell sizes are not seen in *siz1*Δ *siz2*Δ *top1*Δ *rad52*Δ. (C) 2 μm DNA levels in the indicated strains were analyzed by qPCR. Quantities are expressed relative to wt. Error bars, SD. Three independent cultures were analyzed for each sample.

effect on 2 μm accumulation. Whereas the *siz1*Δ *siz2*Δ cir$^+$ mutant was heterogeneous and contained many arrested cells, the *siz1*Δ *siz2*Δ *rad52*Δ *top1*Δ cir$^+$ mutant was not only viable but grew uniformly, similar to the cir° version of this strain (Figure 1, A and B), suggesting that 2 μm may not hyperaccumulate in this mutant. To test whether it was the deletion of *TOP1* that suppressed 2 μm hyperamplification, we examined a *siz1*Δ *siz2*Δ *top1*Δ cir$^+$ mutant and found that it, like *siz1*Δ *siz2*Δ cir$^+$, formed heterogeneous colonies (Figure 1, A and B) and hyperaccumulated 2 μm DNA (Figure 1C). Thus, *top1*Δ does not affect 2 μm accumulation. This result is important for technical reasons, because elimination of *TOP1* suppresses the inviability of *siz1*Δ *siz2*Δ mutants lacking genes of the HRR pathway, thereby permitting us to test whether HRR is involved in 2 μm hyperamplification. Deleting *RAD52* from *siz1*Δ *siz2*Δ *top1*Δ cir$^+$ eliminated both its colony heterogeneity and its 2 μm DNA accumulation (Figure 1). A similar effect on 2 μm DNA levels was seen comparing *siz1*Δ *siz2*Δ cir$^+$ to the barely viable *siz1*Δ *siz2*Δ *rad52*Δ cir$^+$ strain (Figure 1C). This suppression of 2 μm accumulation by *rad52*Δ was not caused by complete loss of 2 μm in most of the

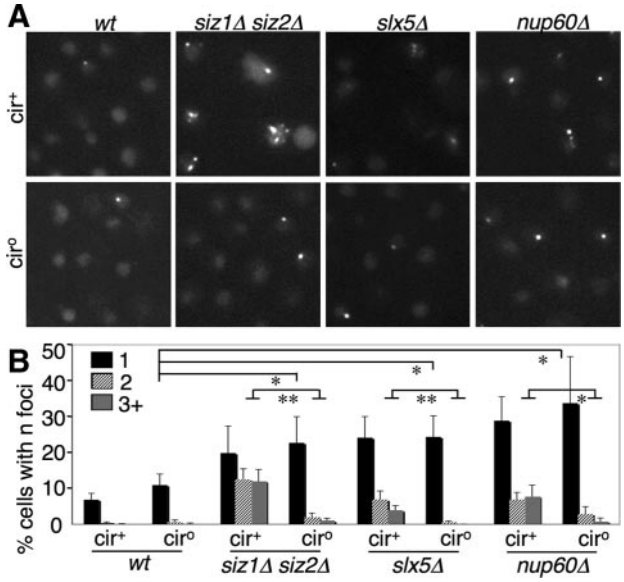


**Figure 2.** Part of the increase in Rad52 foci in SUMO pathway mutants is due to 2 $\mu$m. (A) Cells of the indicated genotype and containing Rad52-GFP were analyzed by fluorescence microscopy. (B) Rad52-GFP foci were counted in cells from triplicate cultures of indicated genotypes. Percent of cells containing 1, 2, or 3+ foci, with SD, is depicted. Statistical significance is given of comparisons between fractions of various cir° strains having one focus, and fractions of cir° and cir$^+$ versions of the same mutant containing $\geq$2 foci. *$p < 0.05$; **$p < 0.01$; calculated using Student's *t* test. n = 700-1500 cells per strain.

population: 7 of 10 *siz1*Δ *siz2*Δ *top1*Δ *rad52*Δ single colonies from Figure 1A were cir$^+$, and the DNA used in Figure 1C was prepared from a similar population (not shown). Thus, *RAD52*-dependent HRR is required for 2 $\mu$m hyperamplification in SUMO pathway mutants. Consistent with this conclusion, accumulation of 2 $\mu$m in *slx5*Δ and *slx8*Δ is also suppressed by deleting *RAD52* (Figure 1C; Burgess *et al.*, 2007).

### *Much of the Increase in Rad52-containing Foci in Sumoylation Mutants Is Related to 2 $\mu$m*

Other labs have reported that SUMO pathway mutants, including *slx5*Δ and *slx8*Δ and the NPC mutants *nup60*Δ, *nup133*Δ, and *nup84*Δ, contain increased levels of Rad52-containing nuclear foci, indicative of elevated ongoing HRR (Burgess *et al.*, 2007; Palancade *et al.*, 2007; Nagai *et al.*, 2008). However, it was not tested to what extent this effect is associated with 2 $\mu$m amplification. We counted Rad52-GFP-containing foci in both cir$^+$ and cir° versions of wt, *siz1*Δ *siz2*Δ, *slx5*Δ, and *nup60*Δ (Figure 2). Mutants containing 2 $\mu$m displayed a ~10-fold increase in the number of cells containing two or more foci, relative to wt. ~80% of this increase was eliminated by removing the 2 $\mu$m from these strains, indicating that most of the increase in cells with multiple foci is due to 2 $\mu$m. However, in the absence of 2 $\mu$m these mutants still showed a two- to threefold increase in the fraction of cells containing a single Rad52-GFP focus. Thus, although much of the increase in Rad52 foci in SUMO pathway mutants is related to hyperamplification of 2 $\mu$m, a significant fraction of the increase involves the chromosomal DNA.

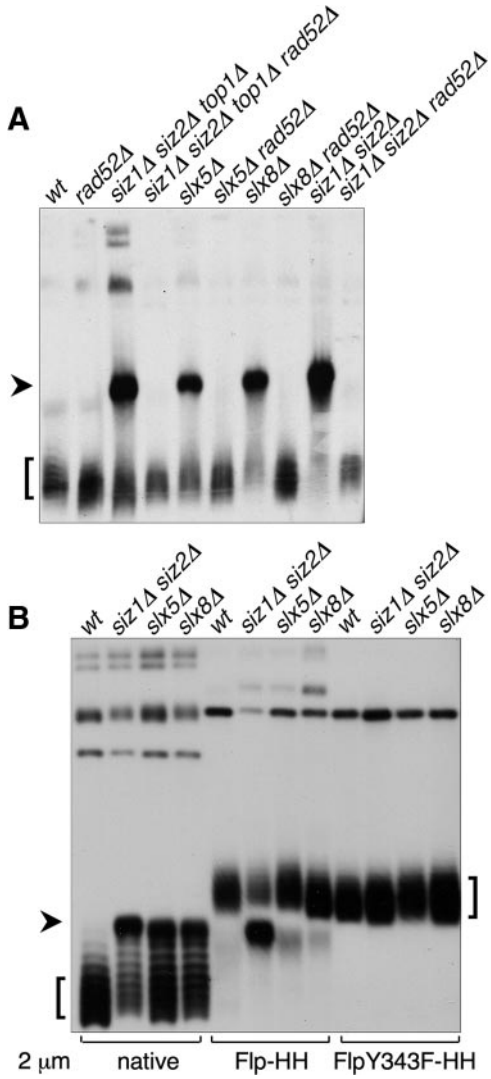


**Figure 3.** Formation of a HMW 2 $\mu$m species in SUMO pathway mutants. (A) Uncut DNA from the indicated strains was analyzed by electrophoresis in an agarose gel containing chloroquine, followed by Southern blotting with a probe against 2 $\mu$m. Lanes were normalized to contain equal amounts of 2 $\mu$m DNA, as measured by qPCR. Arrowhead indicates the aberrant HMW species. Square bracket indicates supercoiled monomeric 2 $\mu$m. (B) DNA from strains of the indicated genotypes containing the indicated versions of 2 $\mu$m were analyzed as in A. Both the Flp-Y343F 2 $\mu$m variant and the corresponding wt control contained a marker gene, and consequently were larger than native 2 $\mu$m. Thus, the supercoiled monomer forms of these plasmids migrated more slowly than native 2 $\mu$m, but the HMW form ran at the same position as for native 2 $\mu$m.

### *SUMO Pathway Mutants Accumulate an Aberrant High-Molecular-Weight Form of 2 $\mu$m*

We next analyzed 2 $\mu$m–containing DNA species in SUMO pathway mutants by Southern analysis of uncut DNA. This experiment showed that *siz1*Δ *siz2*Δ, *siz1*Δ *siz2*Δ *top1*Δ, *slx5*Δ, and *slx8*Δ strains all contained high levels of an aberrant species of 2 $\mu$m (Figure 3A). In conventional agarose gel systems, this species always migrated with the uncut chromosomal DNA, suggesting that it is too large to be resolved in these systems (all DNA >~30 kb migrates at the same rate on these gels; Figure 4A; not shown). Remarkably, this species was not detectable in the corresponding mutant

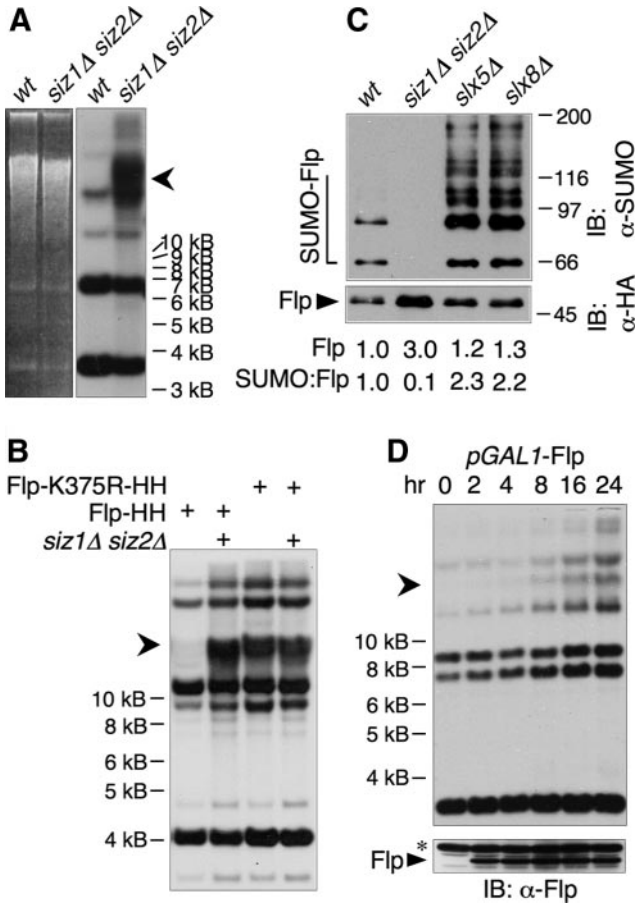


**Figure 4.** Defects in Flp sumoylation lead to formation of the HMW species. (A) Uncut yeast DNA from the indicated strains was analyzed by EtBr-agarose electrophoresis (left) followed by Southern blotting with a probe against 2 μm (right). Lanes contained equal amounts of 2 μm DNA. An arrowhead indicates the HMW form. (B) Uncut DNA from wt or *siz1*Δ *siz2*Δ strains containing the indicated versions of 2 μm was analyzed by Southern blotting as in A. (C) Proteins from indicated strains containing 2 μm expressing Flp(Y343F)-HA-$His_8$ (which does not allow 2 μm amplification) were purified by Ni-NTA affinity chromatography and analyzed by SDS-PAGE and immunoblotting with Abs against SUMO (top) and HA (bottom). Arrowhead indicates unmodified Flp, and an open bracket indicates SUMO-modified Flp. Levels of unmodified Flp as well as ratios of total SUMO signal to unmodified Flp are given below the lanes. Quantities are expressed relative to wt. (D) Flp was expressed from the galactose-inducible *GAL1* promoter for the indicated times in log phase wt cells containing native 2 μm. $A_{600}$ was kept ≤2.0. (top) Uncut DNA was analyzed by Southern blotting as in A, except that lanes contained equal amounts of total DNA rather than equal amounts of 2 μm DNA. (bottom) Whole cell lysates from the same samples as in top panel were analyzed by immunoblotting with an Ab against Flp. Asterisk designates a band that cross-reacts with the Ab.

strains lacking *RAD52*, indicating that its formation requires HRR (Figure 3A). Because 2 μm hyperaccumulation in *siz1*Δ *siz2*Δ depends on Flp activity (Chen *et al.*, 2005), we also analyzed DNA from a strain where 2 μm contained the Flp active site mutant Flp-Y343F (Figure 3B). This experiment showed that Flp activity is also required for accumulation of the high-molecular-weight (HMW) species. In all cases, presence of the HMW species correlated with hyperamplification of 2 μm, suggesting that it may be responsible for 2 μm accumulation. However, the cause-effect relationship between formation of the HMW species and hyperamplification cannot be proven directly.

### *SUMO Attachment to Flp Prevents Accumulation of the HMW Species*

Our previous results have suggested that one mechanism by which the SUMO pathway affects 2 μm DNA levels is through sumoylation of Flp (Chen *et al.*, 2005). Next we asked if reducing SUMO attachment to Flp is sufficient to induce formation of the HMW species. Flp contains one major SUMO attachment site, Lys-375, which when mutated eliminates >90% of Flp sumoylation (Chen *et al.*, 2005). Wild-type yeast containing 2 μm expressing Flp-K375R developed high levels of the HMW species (Figure 4B). Thus, this single mutation in the Flp protein is sufficient to induce formation of the HMW species. This result suggests that Flp that cannot be adequately sumoylated carries out the initiating event in generating the HMW species.

We next asked how the SUMO pathway alters Flp function. We have shown previously that reduction of SUMO attachment to Flp, either using the attachment site mutant or *siz1*Δ *siz2*Δ, results in accumulation of ~3–4-fold higher levels of Flp protein (Chen *et al.*, 2005). Here we examined Flp levels in *slx5*Δ and *slx8*Δ strains as well. Like *siz1*Δ *siz2*Δ, these mutants accumulated somewhat higher levels of Flp protein, but instead of showing reduced sumoylation, these mutants showed dramatically higher levels of SUMO attachment to Flp (Figure 4C). Because these mutants have the same 2 μm–related phenotype as mutants that eliminate Flp sumoylation, this result suggests that Slx5·Slx8 mediates the downstream function of SUMO attachment to Flp (see *Discussion*).

If a simple increase in Flp levels causes the 2 μm hyperamplification in SUMO pathway mutants, overexpression of Flp in wt cells should cause hyperamplification through a similar mechanism. Induction of Flp expression in log phase cells using a galactose-inducible promoter caused 2 μm DNA levels to increase only slowly, with a gradual increase over 24 h (Figure 4D, top), even though proteins expressed from the *GAL1* promoter are induced rapidly, and large amounts of Flp were detected 2 h after induction (Figure 4D, bottom). Amounts of several different 2 μm species increased over this period, including one that comigrated with the chromosomal DNA. However, this form did not accumulate to the levels seen in SUMO pathway mutants, and the other forms increased in similar proportions. While it is difficult to make a direct comparison between this experiment, where Flp levels were increased by orders of magnitude above normal, and SUMO pathway mutants, where Flp levels are increased by a few fold, this result suggests that the effect of SUMO on Flp may be more complex than simply reducing total Flp protein levels.

### *The 2 μm Sequence Is Present in Tandem Arrays in* siz1Δ siz2Δ

We attempted to determine the size of the HMW species using pulsed field gel electrophoresis (see Materials and Methods), but found that much of the 2 μm DNA from *siz1*Δ *siz2*Δ cells was trapped in the well (Figure 5A). This trapped DNA probably represents the HMW species. This result most likely suggests that the HMW species contains structures that inhibit migration of large DNAs, such as large circles, branches, or RFs (Hennessy *et al.*, 1991; Christman *et al.*, 1993; Ma *et al.*, 2008). An alternative explanation, that this effect results from large circular structures becoming entrapped in the well by the agarose in which the DNA had been prepared, can be excluded because the HMW species

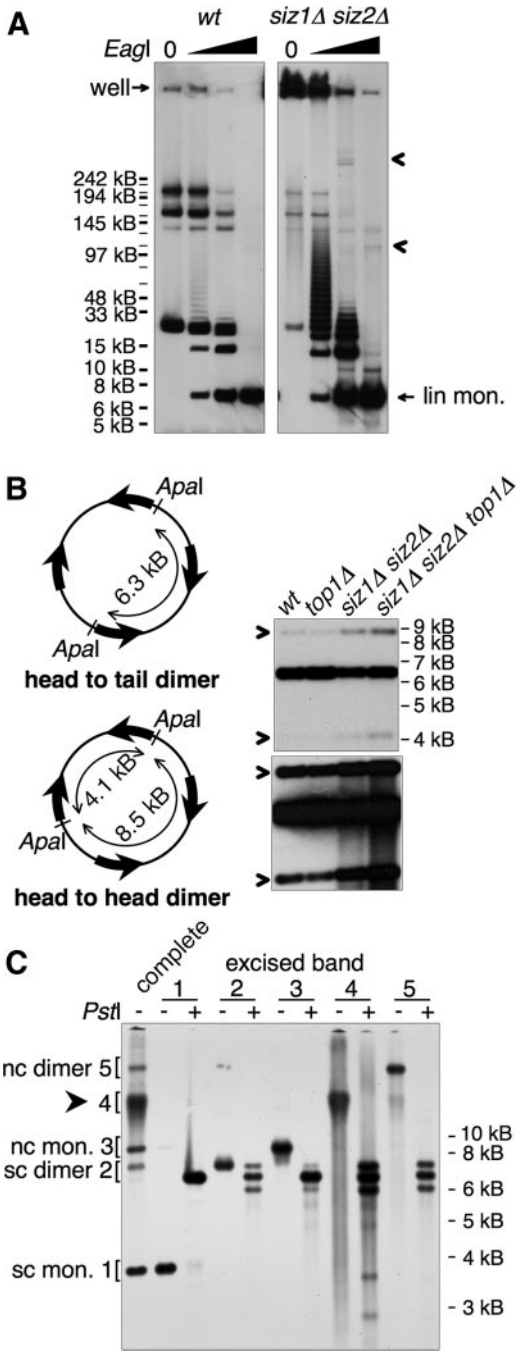


**Figure 5.** The HMW form contains tandem copies of 2 μm. (A) DNA from indicated strains was left untreated or cleaved with increasing amounts of EagI, as indicated, and analyzed by pulsed-field gel electrophoresis, followed by Southern blotting using a probe against 2 μm. All samples were cleaved to completion with BglII, which does not cleave in 2 μm, to reduce chromosomal DNA to small fragments. wt and *siz1*Δ *siz2*Δ panels are from different exposures from the same blot, chosen to normalize the signal from the fully cleaved 2 μm band to the same level, as quantified using the Chemidoc system. The fully cleaved 6.3-kb linear monomer and the position of the well are indicated. Arrowheads designate *siz1*Δ *siz2*Δ-specific low-mobility species released by partial restriction digest that may represent nonlinear portions of the HMW species. Markers were NEB MidRange I, which are all indicated, but not all labeled. Major bands in wt uncut sample probably represent the small circular forms of 2 μm, although this has not been shown directly. (B) Left, illustration of head-to-head and head-to-tail dimer linkages and ApaI restriction fragments. Wide arrows denote the 599-base pair internal repeat sequences that contain FRT. Right, DNA from the indicated strains was digested with ApaI and analyzed by Southern blotting with a probe against 2 μm. Bottom, a darker exposure of the top panel. Bands derived from head-to-head dimer linkages are designated with arrows. (C) The five bands indicated on the left were isolated from an EtBr-stained agarose gel and were either analyzed uncut or were digested with PstI, as indicated, followed by Southern analysis as in Figure 4B. Identities of the 2 μm species are indicated. sc, supercoiled; nc, nicked circular; mon., monomer. Arrowhead designates HMW species.

entered the gel when this agarose-embedded sample was analyzed on a standard agarose gel (Supplemental Figure S1A). (This result does not mean that this species does not contain a circular component.) We next performed partial restriction digests on the DNA using an enzyme that cleaves once in the 2 μm sequence (EagI). For *siz1*Δ *siz2*Δ DNA, this treatment released large amounts of a ladder of 2 μm species extending to >120 kB (Figure 5A). These forms migrated at the expected positions for linear DNAs containing different numbers of copies of the 2 μm sequence, suggesting that the HMW species contains tandem arrays of 2 μm >20 copies long. The wt sample contained only low levels of the smaller forms. In the *siz1*Δ *siz2*Δ samples, restriction digests also released discrete low-mobility 2 μm species (Figure 5A), which may represent portions of the HMW species with nonlinear structures.

When 2 μm DNA isolated from yeast is completely digested with a restriction enzyme that cleaves 2 μm once, three main bands are formed: the 6.3-kb linear monomer, and two forms that are slightly larger and slightly smaller than this. These are formed from "head-to-head" dimeric forms of 2 μm, where the two different Flp-dependent isoforms of 2 μm are linked in tandem (Figure 5B). The size of these forms depends on the position of the restriction site. The 2 μm from *siz1*Δ *siz2*Δ strains contained elevated levels of head-to-head linkages (Figure 5B), suggesting that the HMW species may contain head-to-head linkages. We confirmed this by isolating various 2 μm species and analyzing them separately (Figure 5C). Supercoiled and nicked-circular monomers gave rise to only the 6.3-kb band; whereas the HMW form and the supercoiled and nicked-circular dimers all generated a quantity of the 6.3-kb band that was ~equal to the sum of the higher and lower bands. Thus, these three species contain equal amounts of head-to-head and head-to-tail tandem dimer interactions. This result is consistent with the possibility that the HMW species contains end-to-end copies of the 2 μm sequence.

### *2 μm in* siz1Δ siz2Δ *Contains DSBs near FRT*

The observation that hyperamplification of 2 μm requires *RAD52* suggested that this amplification may occur via repair of DSBs in 2 μm. The restriction analysis of the isolated HMW species also suggested that it may contain DSBs at discrete sites (Figure 5C). Because these breaks in Figure 5C could have been introduced during isolation of this species, we next assayed for DSBs in 2 μm DNA from whole genomic DNA preparations (Figure 6A). This experiment showed that 2 μm DNA from *siz1*Δ *siz2*Δ strains, but not from wt, contains low levels of apparent DSBs at discrete sites. Importantly, these DSBs occur close to the FRT target sites for Flp. As illustrated in Figure 6A, DSBs at one or the other FRT site, combined with restriction enzyme cleavage at a single site, should generate four bands. For Bsu36I, AseI,

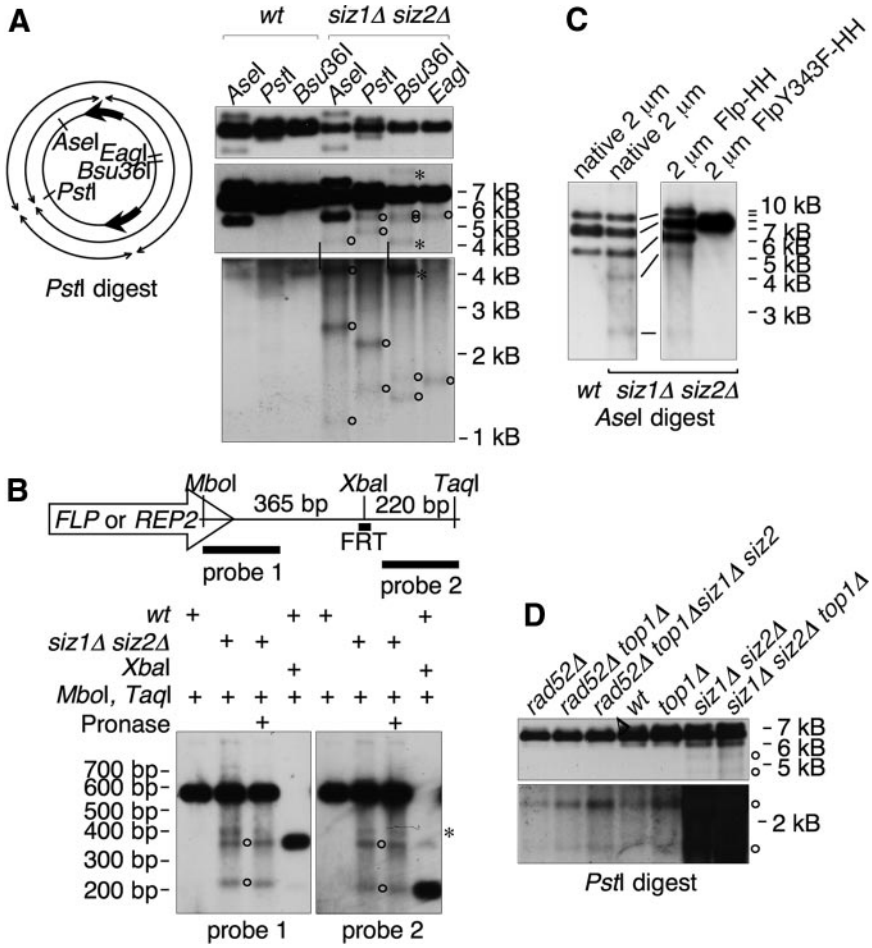


**Figure 6.** The HMW form contains apparent DSBs. (A) Left, diagram of 2 μm monomer showing positions of restriction sites and illustrating the four fragments that would be formed by a PstI digest combined with breaks at FRT. Right, yeast DNA from the indicated strains was digested with indicated restriction enzyme and analyzed by Southern blotting with a probe against 2 μm. All panels are different exposures of the same blot. *siz1*Δ *siz2*Δ samples were slightly underloaded relative to wt. Vertical lines indicate bands that are the same between the middle and bottom panels. Open circles indicate bands representing apparent DSBs near FRT. Asterisks indicate bands that result from incomplete digests. (B) Top, diagram of 599-base pair internal repeat (IR) sequence, showing positions of restriction sites, *FLP/REP2* gene (transcripts from both genes extend into the same side of the IR), FRT, and probes. Flp generates a single-strand break at one of two sites 8 base pairs apart within FRT, and the XbaI site is between these. Bottom, DNA from indicated strains digested with indicated restriction enzymes was analyzed by Southern blotting using the indicated probes (see *Materials and Methods*). Duplicate samples were run on the same gel and blotted, and the blot was cut in half and analyzed with different probes. Some samples were treated with Pronase in an attempt to test whether part of the Flp protein was still attached to these DNAs, but no effect was seen. Circles designate bands that represent DSBs in the IR. The band marked with an asterisk does not appear to represent a DSB, because no corresponding small band is present. We do not know what this band is. (C) DNA from indicated strains containing indicated versions of 2 μm were analyzed as in A. Only two DSB bands are visible with AseI; the other two predicted bands are not visible because one is the same size as the head-to-head dimer band, whereas the other is small and is obscured by background. Panels are from the same exposure of the same blot. (D) DNA from the indicated strains was analyzed as in A. Panels are from different exposures of the same blot.

and EagI, some of the bands were not visible, probably because they were obscured by other bands. However, for PstI, all four bands were visible. Calculations based on band sizes estimated that the breaks are within the inverted repeat sequence ~100 base pairs from FRT, toward the *FLP* and *REP2*-containing side of the plasmid. Experiments to map these breaks more precisely suggested that there are actually DSBs at two sites within the inverted repeat sequence, one at FRT and one ~130 base pairs away toward the *FLP* side of the plasmid (Figure 6B). The most obvious sequence feature near this second site is a poly-(dAdT) sequence. It is not clear why breaks would form at this second site.

The observation that DSBs occur near the FRT sites predicted that formation of these DSBs may depend on Flp activity. This was the case, because a *siz1*Δ *siz2*Δ strain containing 2 μm with inactive Flp did not contain the bands representing DSBs near FRT (Figure 6C). In addition to these discrete bands, the *siz1*Δ *siz2*Δ samples also contained a continuous smear of 2 μm signal that was primarily below the major bands but also continued above them (Figures 5 and 6). This suggests that 2 μm in this mutant contains breaks at random sites and possibly also branched structures or features that inhibit cleavage by restriction enzymes.

The above results suggested a model for 2 μm hyperamplification in which SUMO pathway mutants develop DSBs at or near FRT sites, and that repair of these DSBs by HRR leads to formation of the HMW aberrant species. A simple version of this model would predict that the high levels of DSBs should be present in *siz1*Δ *siz2*Δ even when *RAD52* is absent. However, this was not the case. The *siz1*Δ *siz2*Δ *top1*Δ *rad52*Δ strain contained much lower levels of DSBs than *siz1*Δ *siz2*Δ *top1*Δ, indicating that accumulation of these apparent DSBs depends on *RAD52* (Figure 6D). The critical experiment in testing this hypothesis is the comparison between *top1*Δ *rad52*Δ and *siz1*Δ *siz2*Δ *top1*Δ *rad52*Δ. We also could not detect a clear difference in the amount of these bands between these strains. Thus, these experiments do not support the idea that SUMO mutants contain long-lived Flp-dependent DSBs in the absence of *RAD52*.

### *A Possible Role for BIR in Formation of the HMW Species*

These experiments instead suggest that the apparent DSBs near FRT are a characteristic of the HMW 2 μm species. This might occur if breaks take place primarily within this species. However, an alternative interpretation of these results is that these bands may not represent DSBs, but rather the free ends of a linear portion in the HMW species. This would give a similar band pattern. The model of 2 μm amplification proposed by Futcher would not involve free DNA ends at discrete sites, but other possible mechanisms would. Collision of a RF (or two converging RFs) with a Flp-DNA

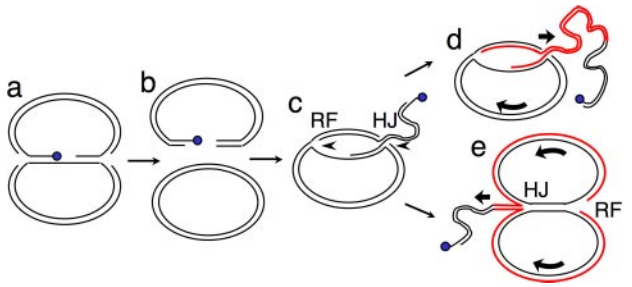


**Figure 7.** Model for formation of 2 $\mu$m rolling circle replication intermediate via BIR. (a) Flp (blue) engaged in a covalent intermediate with DNA at FRT is encountered by one or both replication forks (RFs), resulting in (b) a species containing a DSB where one end has Flp covalently linked to the 3′ end, whereas the other 3′ end is free. (c) The HRR pathway catalyzes invasion of the free 3′ end into an intact circular copy of 2 $\mu$m, generating a new RF. Depending on the mechanism by which BIR occurs (there are several models), the RF could be followed by a Holliday junction (HJ) (shown) or only the 3′end/leading strand could invade, forming a D loop (not shown). (d) Progression of the RF, accompanied by branch migration of the HJ (shown) or progression of the D loop followed by separate lagging strand synthesis (not shown) would give rise to rolling circle replication. (e) If the RF progressed more rapidly than the HJ, it would replicate the circular template until RF progression is impeded by the HJ. RF progression might then promote branch migration of the HJ. Red lines indicate DNA synthesized by the BIR-derived RF. Curved arrows indicate direction of rotation of rolling circle.

covalent intermediate would generate a DSB with Flp covalently bound to the 3′ end on one side (Figure 7). This break might be repaired by BIR: the end of the break with the free 3′ end could invade an intact circular copy of 2 $\mu$m, establishing a rolling circle-like structure, where the RF progresses around the circular template plasmid, generating a linear tail containing tandem copies of 2 $\mu$m. This model predicts that genes involved in BIR should be required for formation of the HMW species. We found that *siz1*Δ *siz2*Δ *top1*Δ mutants also lacking singly any of *RAD50*, *RAD51*, *RAD54*, *RAD55*, *RAD57*, *RAD59*, *RDH54/TID1*, or *XRS2* all still contained the HMW species, unlike the corresponding *rad52*Δ mutant, which entirely lacks this species (Figure 8A; Supplemental Figure S1B). Next we quantified the relative level of the HMW species in a subset of these mutants as well as in *rad51*Δ *rad59*Δ and *rad54*Δ *rdh54*Δ double mutants, which eliminate the two known BIR pathways, and in *pol32*Δ, which lacks a subunit of DNA polymerase δ that is required for *RAD51*-dependent BIR (Lydeard *et al.*, 2007). This experiment showed ~50% reductions of the HMW species in *pol32*Δ and in the *rad51*Δ *rad59*Δ and *rad54*Δ *rdh54*Δ double mutants (Figure 8A). The reduction in the *rad59*Δ single mutant was also significant. Thus, the genes involved in known BIR pathways are partially responsible for the amplification of 2 $\mu$m in *siz1*Δ *siz2*Δ mutants (see *Discussion*).

The model that 2 $\mu$m hyperamplification is initiated by a DSB containing covalently bound Flp also suggests that mutants that hyperamplify 2 $\mu$m might contain elevated levels of Flp covalently bound to DNA. However, we were unable to detect this covalent intermediate (not shown).

We were also interested in whether the HMW species consists of a continuously replicating species that might contain active RFs outside of normal S phase, or whether it comprises mostly dead-end products that are replicated only during S phase. Analysis of DNA isolated from cells that had been arrested in G2/M by treatment with nocodazole or

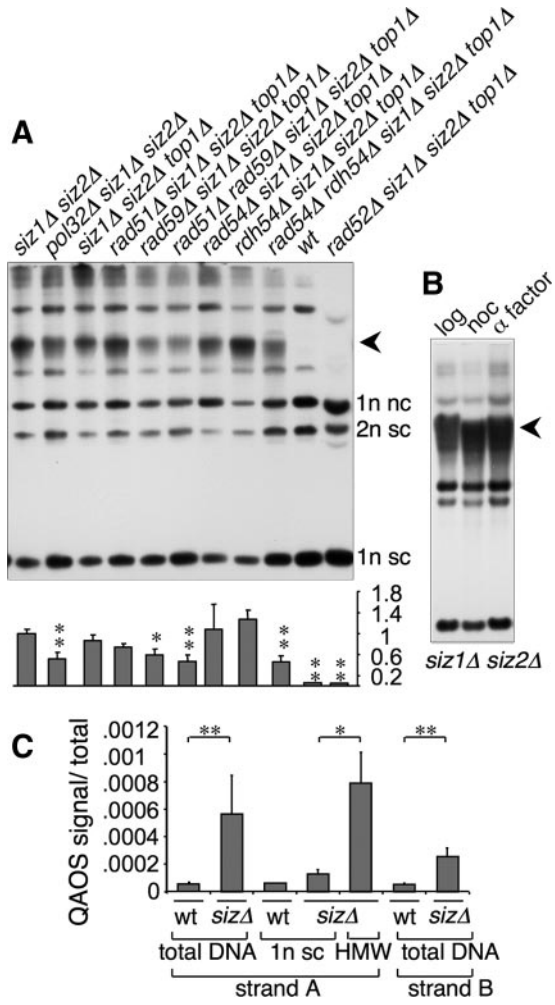


**Figure 8.** Genes involved in BIR contribute to formation of the HMW species, which contains ssDNA. (A) Top, uncut DNA from the indicated strains was analyzed by Southern blotting with a probe against 2 $\mu$m. Lanes were normalized to contain equal quantities of 2 $\mu$m DNA. Arrowhead indicates HMW species. Bottom, graph of the ratio of the HMW species to the sum of the two monomeric species plus the supercoiled dimer species. Ratios are relative to *siz1*Δ *siz2*Δ. Three independent experiments were averaged, and SD is given. *siz1*Δ *siz2*Δ *pol32*Δ was compared with *siz1*Δ *siz2*Δ; other strains to *siz1*Δ *siz2*Δ *top1*Δ. *$p < 0.02$; **$p < 0.01$; calculated using Student's *t* test. (B) Uncut DNA isolated from *siz1*Δ *siz2*Δ cells in log phase (log), after 4-h nocodazole treatment (noc) or after 3-h nocodazole treatment followed by 3-h α factor treatment (α factor) was analyzed as in A. (C) Levels of ssDNA in the indicated DNA preparations was measured using QAOS (see *Materials and Methods*). Ratio of QAOS signal to total DNA at the same locus is given. "*siz*Δ" is *siz1*Δ *siz2*Δ; "1n sc" is isolated supercoiled 2 $\mu$m monomer; "HMW" is isolated DNA from the main chromosomal DNA band, which contains the HMW 2 $\mu$m species. Three independent DNA preparations were assayed for each sample, except for the isolated supercoiled monomer from wt cells, where two preparations were used. Error bars, SD, except for wt sc monomer where no error is given. *$p < 0.05$; **$p < 0.01$; calculated using Student's *t* test.

in G1 with α factor showed that the HMW species persists through the cell cycle (Figure 8B). We next tested for ongoing replication of 2 $\mu$m during nocodazole arrest but were unable to detect incorporation of bromodeoxyuridine (BrdU) into 2 $\mu$m DNA in nocodazole-arrested cells (Sup-

plemental Figure S1C). These results suggest that at least most of the HMW species is not a continuously replicating rolling circle.

### *The HMW Species contains ssDNA*

One prediction of the BIR model proposed here is that the HMW species might contain ssDNA. This is because the 5′ ends of DSBs or free ends are resected by exonucleases to produce a single-stranded 3′ tail for strand invasion during HRR (Harrison and Haber, 2006). Replication intermediates also contain ssDNA. To quantify ssDNA in 2 μm, we used the PCR-based locus-specific QAOS method (quantitative analysis of ssDNA; Booth *et al.*, 2001; see *Materials and Methods*; Supplemental Figure S2). This experiment showed that the fraction of the tested site in 2 μm DNA that is single-stranded in *siz1*Δ *siz2*Δ is ~5–10-fold higher than in wt. ssDNA was elevated on both strands (see *Materials and Methods*). More importantly, the level of ssDNA was about sixfold higher in the HMW species than in *siz1*Δ *siz2*Δ-derived supercoiled monomer. Thus, the HMW species contains elevated levels of ssDNA. Because ssDNA activates checkpoint signaling (Harrison and Haber, 2006), this result provides a possible explanation for why SUMO pathway mutants exhibit 2 μm–dependent checkpoint-mediated cell cycle delays.

## DISCUSSION

Our data suggest that SUMO attachment to Flp recombinase prevents Flp from causing DNA damage. We propose that when Flp is not sumoylated, Flp-dependent damage is repaired by the cellular HRR pathway, ultimately leading to formation of a HMW species containing multiple tandem copies of the 2 μm sequence. This aberrant process is associated with the elevated levels of 2 μm DNA in SUMO pathway mutants. There is no reason to think that normal Flp-dependent 2 μm amplification in wt cells occurs by the same mechanism. The SUMO pathway could also affect 2 μm behavior via additional mechanisms.

The effect of SUMO on Flp appears to be mediated by Slx5·Slx8. The most likely explanation for this is that Slx5·Slx8 targets sumoylated Flp for ubiquitin-dependent proteolysis. However, we have not been able to detect a difference in the levels of Flp ubiquitylation or degradation between wt and *siz1*Δ *siz2*Δ or *slx5*Δ or *slx8*Δ mutants, using overexpressed Flp (not shown). One explanation for this would be if Flp can be ubiquitylated and degraded via multiple pathways, where SUMO-dependent degradation accounts for a relatively small fraction, at least when Flp is overexpressed. For example, SUMO- and Slx5·Slx8-dependent ubiquitylation might target only DNA-bound Flp. This model would explain the result that Flp causes DNA damage in SUMO pathway mutants, because increased residence of Flp at the DNA would increase the chance that the Flp-DNA covalent intermediate would be encountered by a RF and converted to a double-strand break. This model would also explain why overexpression of Flp in wt cells did not have the same effect as reducing Flp sumoylation (Figure 4), because overexpressed Flp could still be removed from the DNA by the SUMO pathway.

Several observations suggest that amplification of 2 μm in SUMO pathway mutants may occur via BIR (Figures 5, 6, and 8). However, BIR mutants such as *rad51*Δ *rad59*Δ had only an approximately twofold effect on levels of the HMW species, indicating that the two known BIR pathways (*RAD51*-dependent and *RAD51*-independent) are not absolutely required for formation of the HMW species. This could suggest 1) that BIR is occurring through a third mechanism, 2) that the requirements for BIR are relaxed when 2 μm is the template, or 3) that the HMW species can form by a mechanism other than BIR. *rad51*Δ *rad59*Δ and *rad54*Δ *rdh54*Δ eliminate most, but not all, BIR (McEachern and Haber, 2006; Llorente *et al.*, 2008), indicating that there are BIR mechanisms that do not require these pairs of genes. Furthermore, the presence of a circular template might reduce the need for some features of the BIR mechanism. There are several models for how BIR takes place, some of which involve formation of a Holliday junction (HJ) behind the RF (McEachern and Haber, 2006; Llorente *et al.*, 2008). This HJ could either be resolved or could branch-migrate behind the RF. BIR on a circular template would not require either of these mechanisms to deal with the HJ, because the RF could travel around the template until it came up behind the HJ, where it might "push" branch migration of the HJ (Figure 7E). A non-BIR mechanism could also produce the structure in Figure 7E: during plasmid replication, one RF could stall at Flp-bound FRT and regress, forming a "chicken foot" HJ-like structure. If the fork from the other side of the plasmid then passed the FRT site, it might push this regressed fork/HJ backward, extruding a linear tail, where the end represents the site where the fork initially stalled. If the HMW species were formed this way, the end would not be precisely at the Flp cleavage site in FRT, but would be nearby.

Another model that would explain formation of tandem copies of the 2 μm DNA sequence is the double rolling circle model (Futcher, 1986). However, this model does not account for the presence of apparent DSBs near FRT or for the participation of the HRR pathway in 2 μm hyperamplification in SUMO mutants. Both the single and double rolling circle models predict formation of primarily head-to-tail linkages between the tandem copies of 2 μm, if the circular template is a 2 μm monomer. This contrasts with our observation of equal levels of head-to-head and head-to-tail linkages in the HMW species. This discrepancy could be explained either if the template circle is a dimer or larger or if Flp activity randomizes the linkages after formation of the tandem multimer.

We did not detect evidence of ongoing replication of 2 μm in G2/M-arrested cells, suggesting that high levels of active RFs are not present in 2 μm throughout the cell cycle. The rolling circle intermediate proposed here could meet several fates. One is that Flp-dependent recombination between the circle and the tail could redirect the RF, and any HJ, off the end of the tail, generating a linear molecule. There could also be a cellular mechanism that destroys residual RFs late in the cell cycle. The absence of high levels of ongoing replication is consistent with a model where initiation of 2 μm hyperamplification is relatively rare, but that the aberrant species formed is replicated every cell cycle during S phase, so that the species persists in lineages where it develops. This model is consistent with the "nibbled" colony growth of $cir^+$ SUMO pathway mutants, where some $cir^+$ lineages grow well for many generations, indicating that these cells only rarely generate the species that causes growth arrest (Dobson *et al.*, 2005). The species predicted by our model would trigger checkpoint responses even if they are replicated only during S phase, because they would contain free ends without telomeres.

The SUMO pathway has complex effects on genome stability in *S. cerevisiae* and directly affects diverse aspects of DNA metabolism, including DNA repair (Geiss-Friedlander and Melchior, 2007). However, our work suggests that for 2 μm, the major effect of the SUMO pathway is to prevent

Flp-dependent DNA damage, not to regulate the repair mechanism, as has been proposed (Burgess *et al*., 2007). There is a slight discrepancy between our results, showing that mutants such as *rad59*Δ have a modest effect on accumulation of the HMW species in *siz1*Δ *siz2*Δ *top1*Δ (Figure 8), and a previous result showing that these mutants strongly suppress the 2 μm–related colony growth defects of the *slx8*Δ mutant (Burgess *et al*., 2007). It is likely that this discrepancy is explained by complete loss of 2 μm in the *slx8*Δ experiment. In our hands, *slx5*Δ and *slx8*Δ strains rapidly self-select for loss of 2 μm (not shown). *rad59*Δ also increased 2 μm loss in *siz1*Δ *siz2*Δ *top1*Δ (not shown). These observations emphasize the importance of using cir° versions of these SUMO pathway mutants for most experiments. Not only do cir$^+$ versions of these mutants show apparent genome instability phenotypes that are actually secondary effects of 2 μm accumulation (Figure 2), but they also display confusing effects resulting from spontaneous loss of the plasmid. Crossing the resulting cir° mutants to cir$^+$ strains accentuates this confusion because it generates mutant segregants that have, at least temporarily, reacquired 2 μm and therefore grow more poorly than the parental cir° strain.

## ACKNOWLEDGMENTS

We thank M. Jayaram for the α-Flp Ab and J. Diffley (Cancer Research UK) for plasmids. We also thank M. Adkins for advice on chloroquine gels and E. Wickstrom, C. Scott, M. King, and E. Alnemri for use of their equipment. H.R.S. was supported by National Research Service Award T32-DK07705. This work was supported in part by MCB-0820228 from the National Science Foundation and in part by a Reapplication Enhancement Award from Thomas Jefferson University.

## REFERENCES

Adkins, M. W., and Tyler, J. K. (2004). The histone chaperone Asf1p mediates global chromatin disassembly in vivo. J. Biol. Chem. *279*, 52069–52074.

Ausubel, F. M., Brent, R., Kingston, R. E., Moore, D. D., Smith, J. A., Seidman, J. G., and Struhl, K. (2000). Current Protocols in Molecular Biology, New York: Wiley-Interscience.

Booth, C., Griffith, E., Brady, G., and Lydall, D. (2001). Quantitative amplification of single-stranded DNA (QAOS) demonstrates that *cdc13-1* mutants generate ssDNA in a telomere to centromere direction. Nucleic Acids Res. *29*, 4414–4422.

Broach, J. R., and Volkert, F. C. (1991). Circular DNA plasmids of yeasts. In: The Molecular and Cellular Biology of the Yeast *Saccharomyces*, Vol. 1, ed. J. R. Broach, E. W. Jones, and J. R. Pringle, Plainview, NY: Cold Spring Harbor Press, 297–331.

Burgess, R. C., Rahman, S., Lisby, M., Rothstein, R., and Zhao, X. (2007). The Slx5-Slx8 complex affects sumoylation of DNA repair proteins and negatively regulates recombination. Mol. Cell. Biol. *27*, 6153–6162.

Chen, X. L., Reindle, A., and Johnson, E. S. (2005). Misregulation of 2 μm circle copy number in a SUMO pathway mutant. Mol. Cell. Biol. *25*, 4311–4320.

Chen, X. L., Silver, H. R., Xiong, L., Belichenko, I., Adegite, C., and Johnson, E. S. (2007). Topoisomerase I-dependent viability loss in *Saccharomyces cerevisiae* mutants defective in both SUMO conjugation and DNA repair. Genetics *177*, 17–30.

Christman, M. F., Dietrich, F. S., Levin, N. A., Sadoff, B. U., and Fink, G. R. (1993). The rRNA-encoding DNA array has an altered structure in topoisomerase I mutants of *Saccharomyces cerevisiae*. Proc. Natl. Acad. Sci. USA *90*, 7637–7641.

Dobson, M. J., Pickett, A. J., Velmurugan, S., Pinder, J. B., Barrett, L. A., Jayaram, M., and Chew, J. S. (2005). The 2 μm plasmid causes cell death in *Saccharomyces cerevisiae* with a mutation in Ulp1 protease. Mol. Cell. Biol. *25*, 4299–4310.

Futcher, A. B. (1986). Copy number amplification of the 2 micron circle plasmid of *Saccharomyces cerevisiae*. J. Theor. Biol. *119*, 197–204.

Geiss-Friedlander, R., and Melchior, F. (2007). Concepts in sumoylation: a decade on. Nat. Rev. Mol. Cell Biol. *8*, 947–956.

Grainge, I., and Jayaram, M. (1999). The integrase family of recombinase: organization and function of the active site. Mol. Microbiol. *33*, 449–456.

Harrison, J. C., and Haber, J. E. (2006). Surviving the breakup: the DNA damage checkpoint. Annu. Rev. Genet. *40*, 209–235.

Hay, R. T. (2005). SUMO: a history of modification. Mol. Cell *18*, 1–12.

Hennessy, K. M., Lee, A., Chen, E., and Botstein, D. (1991). A group of interacting yeast DNA replication genes. Genes Dev. *5*, 958–969.

Hoffman, C. S., and Winston, F. (1987). A ten-minute DNA preparation from yeast efficiently releases autonomous plasmids for transformation of *Escherichia coli*. Gene *57*, 267–272.

Holm, C., Meeks-Wagner, D. W., Fangman, W. L., and Botstein, D. (1986). A rapid, efficient method for isolating DNA from yeast. Gene *42*, 169–173.

Ii, T., Fung, J., Mullen, J. R., and Brill, S. J. (2007a). The yeast Slx5-Slx8 DNA integrity complex displays ubiquitin ligase activity. Cell Cycle *6*, 2800–2809.

Ii, T., Mullen, J. R., Slagle, C. E., and Brill, S. J. (2007b). Stimulation of in vitro sumoylation by Slx5-Slx8, evidence for a functional interaction with the SUMO pathway. DNA Repair *6*, 1679–1691.

Jayaram, M., Mehta, S., Uzri, D., Voziyanov, Y., and Velmurugan, S. (2004). Site-specific recombination and partitioning systems in the stable high copy propagation of the 2-micron yeast plasmid. Prog. Nucleic Acid. Res. Mol. Biol. *77*, 127–172.

Johnson, E. S. (2004). Protein modification by SUMO. Annu. Rev. Biochem. *73*, 355–382.

Johnson, E. S., and Blobel, G. (1999). Cell cycle-regulated attachment of the ubiquitin-related protein SUMO to the yeast septins. J. Cell Biol. *147*, 981–994.

Koster, D. A., Palle, K., Bot, E. S., Bjornsti, M. A., and Dekker, N. H. (2007). Antitumour drugs impede DNA uncoiling by topoisomerase I. Nature *448*, 213–217.

Krogh, B. O., and Symington, L. S. (2004). Recombination proteins in yeast. Annu. Rev. Genet. *38*, 233–271.

Lewis, A., Felberbaum, R., and Hochstrasser, M. (2007). A nuclear envelope protein linking nuclear pore basket assembly, SUMO protease regulation, and mRNA surveillance. J. Cell Biol. *178*, 813–827.

Li, T. K., and Liu, L. F. (2001). Tumor cell death induced by topoisomerase-targeting drugs. Annu. Rev. Pharmacol. Toxicol. *41*, 53–77.

Llorente, B., Smith, C. E., and Symington, L. S. (2008). Break-induced replication: what is it and what is it for? Cell Cycle *7*, 859–864.

Lydeard, J. R., Jain, S., Yamaguchi, M., and Haber, J. E. (2007). Break-induced replication and telomerase-independent telomere maintenance require Pol32. Nature *448*, 820–823.

Ma, W., Resnick, M. A., and Gordenin, D. A. (2008). Apn1 and Apn2 endonucleases prevent accumulation of repair-associated DNA breaks in budding yeast as revealed by direct chromosomal analysis. Nucleic Acids Res. *36*, 1836–1846.

McEachern, M. J., and Haber, J. E. (2006). Break-induced replication and recombinational telomere elongation in yeast. Annu. Rev. Biochem. *5*, 111–135.

Mumberg, D., Muller, R., and Funk, M. (1994). Regulatable promoters of *Saccharomyces cerevisiae*: comparison of transcriptional activity and their use for heterologous expression. Nucleic Acids Res. *22*, 5767–5768.

Murray, J. A., Scarpa, M., Rossi, N., and Cesareni, G. (1987). Antagonistic controls regulate copy number of the yeast 2 mu plasmid. EMBO J. *6*, 4205–4212.

Nagai, S., Dubrana, K., Tsai-Pflugfelder, M., Davidson, M. B., Roberts, T. M., Brown, G. W., Varela, E., Hediger, F., Gasser, S. M., and Krogan, N. J. (2008). Functional targeting of DNA damage to a nuclear pore-associated SUMO-dependent ubiquitin ligase. Science *322*, 597–602.

Palancade, B., Liu, X., Garcia-Rubio, M., Aguilera, A., Zhao, X., and Doye, V. (2007). Nucleoporins prevent DNA damage accumulation by modulating Ulp1-dependent sumoylation processes. Mol. Biol. Cell *18*, 2912–2923.

Paques, F., and Haber, J. E. (1999). Multiple pathways of recombination induced by double-strand breaks in *Saccharomyces cerevisiae*. Microbiol. Mol. Biol. Rev. *63*, 349–404.

Pommier, Y. (2006). Topoisomerase I inhibitors: camptothecins and beyond. Nat. Rev. Cancer *6*, 789–802.

Prado, F., Gonzalez-Barrera, S., and Aguilera, A. (2000). RAD52-dependent and -independent homologous recombination initiated by Flp recombinase at a single FRT site flanked by direct repeats. Mol. Gen. Genet. *263*, 73–80.

Prudden, J., Pebernard, S., Raffa, G., Slavin, D. A., Perry, J. J., Tainer, J. A., McGowan, C. H., and Boddy, M. N. (2007). SUMO-targeted ubiquitin ligases in genome stability. EMBO J. *26*, 4089–4101.

Reynolds, A. E., Murray, A. W., and Szostak, J. W. (1987). Roles of the 2 microns gene products in stable maintenance of the 2 microns plasmid of *Saccharomyces cerevisiae*. Mol. Cell. Biol. *7*, 3566–3573.

Schwartz, D. C., and Cantor, C. R. (1984). Separation of yeast chromosome-sized DNAs by pulsed field gradient gel electrophoresis. Cell *37*, 67–75.

Sherman, F., Fink, G. R., and Hicks, J. B. (1986). Methods in Yeast Genetics, Cold Spring Harbor, NY: Cold Spring Harbor Laboratory Press.

Storici, F., and Bruschi, C. V. (2000). Involvement of the inverted repeat of the yeast 2-micron plasmid in Flp site-specific and *RAD52*-dependent homologous recombination. Mol. Gen. Genet. *263*, 81–89.

Sun, H., Leverson, J. D., and Hunter, T. (2007). Conserved function of RNF4 family proteins in eukaryotes: targeting a ubiquitin ligase to SUMOylated proteins. EMBO J. *26*, 4102–4112.

Uzunova, K., *et al.* (2007). Ubiquitin-dependent proteolytic control of SUMO conjugates. J. Biol. Chem. *282*, 34167–34175.

Xie, Y., Kerscher, O., Kroetz, M. B., McConchie, H. F., Sung, P., and Hochstrasser, M. (2007). The yeast Hex3·Slx8 heterodimer is a ubiquitin ligase stimulated by substrate sumoylation. J. Biol. Chem. *282*, 34176–34184.

Yaffe, M. P., and Schatz, G. (1984). Two nuclear mutations that block mitochondrial protein import in yeast. Proc. Natl. Acad. Sci. USA *81*, 4819–4823.

Zhao, X., Wu, C. Y., and Blobel, G. (2004). Mlp-dependent anchorage and stabilization of a desumoylating enzyme is required to prevent clonal lethality. J. Cell Biol. *167*, 605–611.